Supporting Information

Facile High-Yield Solvothermal Deposition of Inorganic Nanostructures on Zeolite Crystals for Mixed Matrix Membrane Fabrication

Tae-Hyun Bae, Junqiang Liu, Jong Suk Lee,
William J. Koros, Christopher W. Jones, and Sankar Nair

School of Chemical & Biomolecular Engineering, Georgia Institute of Technology
311 Ferst Drive, Atlanta, Georgia 30332-0100

Materials and Methods

Materials

The following chemicals were commercially available and were used as received: tetraethylorthosilicate (TEOS, 98% Sigma-Aldrich), tetrapropylammonium hydroxide (TPAOH, 40% w/w aqueous solution, Alfa Aesar), tetrapropylammonium bromide (TPABr, 98%, Sigma-Aldrich), ethylenediamine (99%, Sigma-Aldrich), methylmagnesium bromide (3M in ether, Sigma-Aldrich), 2-propanol (Sigma-Aldrich), dichloromethane (DCM, 99.5%, Sigma-Aldrich), toluene (99.8%, Sigma-Aldrich), magnesium sulfate heptahydrate (Acros) and sodium chloride (Fisher Scientific).

Synthesis of Pure silica MFI

Pure silica MFI crystals were synthesized hydrothermally at 150°C from TEOS/TPAOH/water solutions. The TEOS/TPAOH molar ratio was 1:0.36 or 1:0.24 and the water content was varied from 20 to 360 on a molar basis as part of a synthesis matrix that included variation in the reaction time (2 to 4 days). The general methodology otherwise followed that described in our previous work[1]. Large crystal MFI was also prepared using the method described in the literature[2]. The solution with molar ratio of 1TEOS: 0.1TPABr:0.1NaOH:98H_2O was aged at 50°C for 7days and crystallized at 120°C for 2days.

Grignard treatment

After dispersing 0.5 g of pure silica MFI in 3M aqueous NaCl solution, the suspension was filtered using microfiltration membrane with 0.1μm pores to collect the particles. To remove residual water, particles were dried at 80°C overnight. The NaCl seeded particles were placed in round bottom flask and 8 ml of toluene was added. After adding 1.5ml of 3M CH_3MgBr in ether,

the suspension was sonicated for 4hr and then stirred at room temperature for 12hr. 2-propanol was added dropwise to quench the Grignard reagent and the mixture was centrifuged to collect the particles. To remove residual solvents, the particles were washed with 2-propanol several times. After that, 40 ml of DI water was added to the particles and the mixture was sonicated for 2hr. The particles were washed with DI water by several repetitions of sonication and centrifugation, and were finally dried at 80°C.

Solvothermal treatment

After dispersing 0.2 g of pure silica MFI in 10 ml of ethylenediamine by sonication, 1 ml of 1M $MgSO_4$ aqueous solution was added dropwise to the dispersion while applying vigorous stirring. After further stirring for 1hr, the mixture was transferred to a Teflon-lined autoclave and solvothermal treatment was performed at 160°C in an oven for 12 hr. The particles were washed with DI water by several repetitions of sonication and centrifugation and dried at 80°C.

Mixed matrix membrane fabrication

Mixed matrix membranes were prepared using a solution-casting technique. Zeolite particles were dispersed in DCM using a sonication horn. After that, a poly(etherimide) (Ultem® 1000, GE Plastics) or Matrimid® (Vantico Inc.) was added to the suspension and the solution was stirred overnight. After pouring the solution on a glass plate, a nascent film was cast with a "doctor's knife". Finally, a dense film was obtained after drying at room temperature. All membranes were annealed at 230°C for 12 hr prior to gas permeation tests.

Characterization

Morphologies of both zeolite particles and mixed matrix membranes were observed with a scanning electron microscope (SEM, LEO 1530). To prevent any morphological change, zeolite particles were observed without coating with gold. On the other hand, to observe cross-sections, mixed matrix membranes were coated with gold after being cryogenically fractured in liquid nitrogen. Energy dispersive X-ray spectroscopy (EDS) was used to investigate the elemental composition of zeolites. Bulk compositions were also measured with ICP-AES (inductively coupled plasma atomic emission spectroscopy) with an outside vendor, Columbia Analytical Services Inc. Micropore volume by t-plot method and BET (Brunauer-Emmett-Teller) surface area were calculated from nitrogen physisorption measurements performed on a Micromeritics ASAP 2020 or 2010. Powder X-ray diffraction (XRD) patterns were obtained on a Philips X'pert diffractometer equipped with X'celerator using Cu Kα radiation. Differential scanning calorimetry (DSC) was performed on a Netzsch STA409. Samples were initially heated under a nitrogen-diluted air stream from 30°C to 300°C at 10 °C/min and cooled to room temperature.

DSC curves were obtained during the second run at a heating rate of 10 °C/min.

Permeation tests

Single gas permeation tests were performed in a constant volume apparatus. In the system, feed and permeate reservoirs were separated by a cell that holds the membrane. It includes appropriate instrumentation for measuring the pressure in both reservoirs and necessary valves, all within a constant temperature box. The detailed experimental procedure is described in the literature[3]. Permeation tests were performed with 2.0 or 4.5 atm upstream pressure at 35°C. Numerous measurements were performed for the thickness of each sample by using a micrometer, and their arithmetic average values were used for permeation data analysis.

Theoretical prediction of uncalcined MFI/Ultem® membrane performance

The permeabilities of gases in mixed matrix membranes with ideal morphology can be estimated by the Maxwell model[4,5] if the permeabilities of the individual constituents of the membrane are known. Since the uncalcined MFI is non-porous, oxygen and nitrogen permeabilities in uncalcined MFI are exactly zero. The permeabilities in polymer phase were obtained from the permeation tests of a pure Ultem® dense film. A modified-Maxwell model, which is a three-phase (polymer, sieve and voids) Maxwell model, was utilized to predict the performance of the above mixed matrix membranes[4,5].

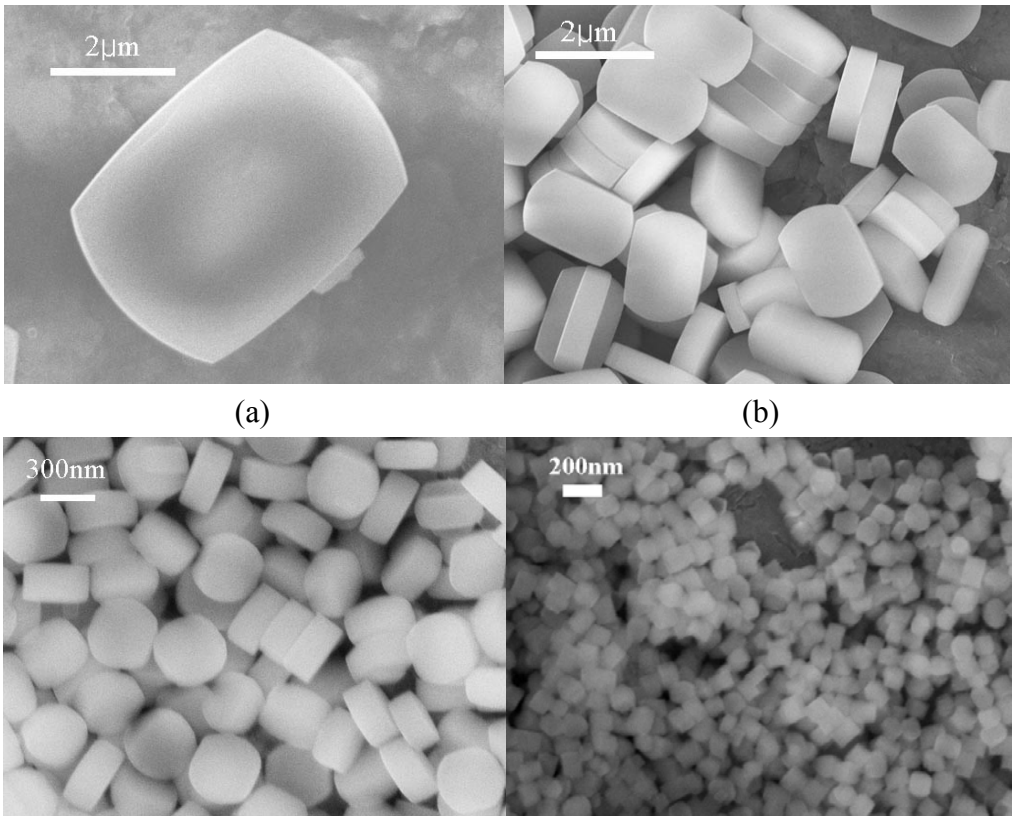

Fig. S1. SEM images of pure-silica-MFI particles; (a) 5 μm large crystal; (b)-(c) crystals synthesized from the precursor solution composition of 1 TEOS: *x* TPAOH: *y* H_2O for *z* days. (b) 2 μm, *x* = 0.24, *y* = 360 and *z* = 4; (c) 300 nm, *x* = 0.36, *y* = 180 and *z* = 2; (d) 100 nm, *x* = 0.36, *y* = 20 and *z* = 4. The maximum size of large the crystals made using TPABr was approximately 5μm but particles showed a broad size distribution. In contrast, crystals synthesized with TPAOH as the structure directing agent (SDA) showed uniform sizes. 100 nm, 300 nm and 2 μm crystals were synthesized by adjusting the reaction conditions such as the reaction time and the amount of SDA or water.

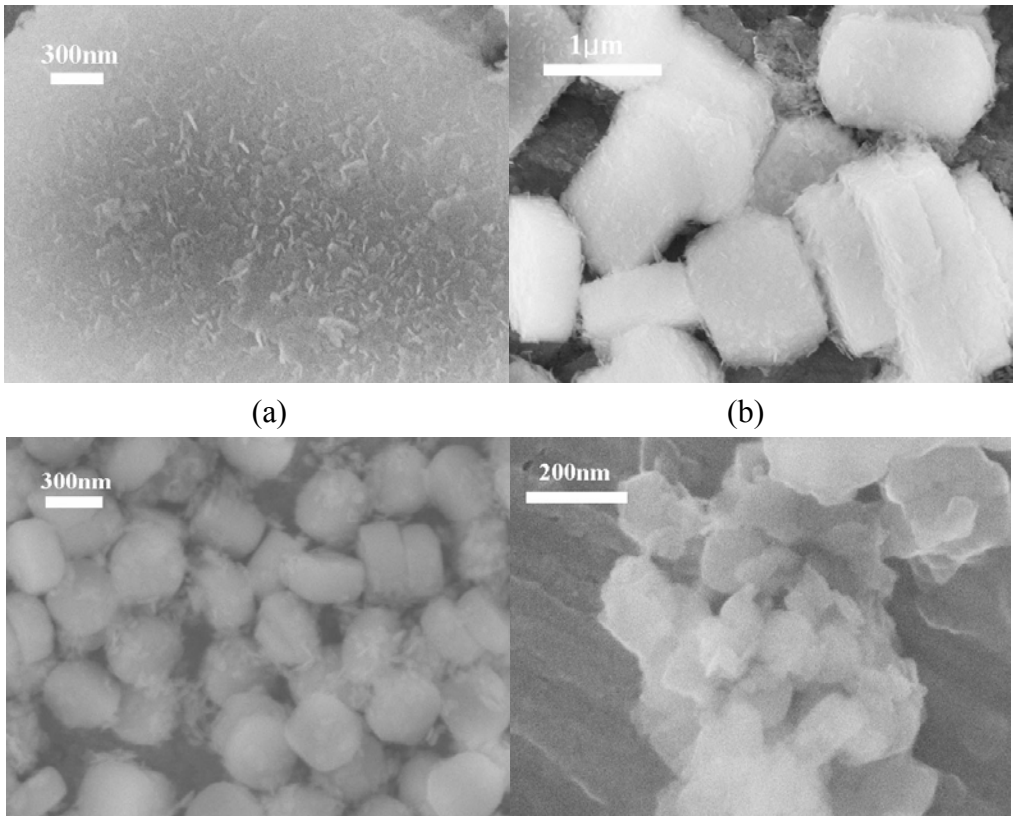

Fig. S2. SEM images of pure-silica-MFI treated with Grignard reagent; (a) 5 μm, (b) 2 μm, (c) 300 nm and (d) 100 nm crystals. Roughened surfaces were created by the formation of whisker and platelet shaped crystals on the surface of the MFI. In the case of 100 nm MFI, the surfaces were coated with a much finer layer of magnesium hydroxide. In addition, particle aggregation upon drying was more significant compared to larger MFI particles.

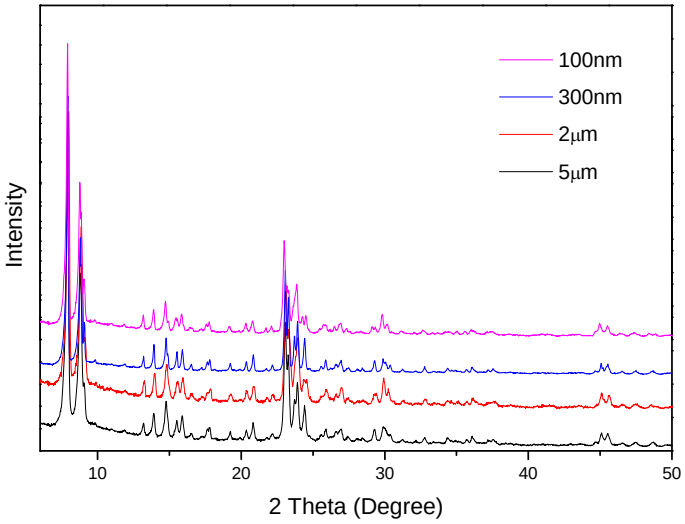

Fig. S3. Powder XRD patterns of pure-silica-MFI particles. All synthesized crystals exhibited the structure of zeolite MFI.

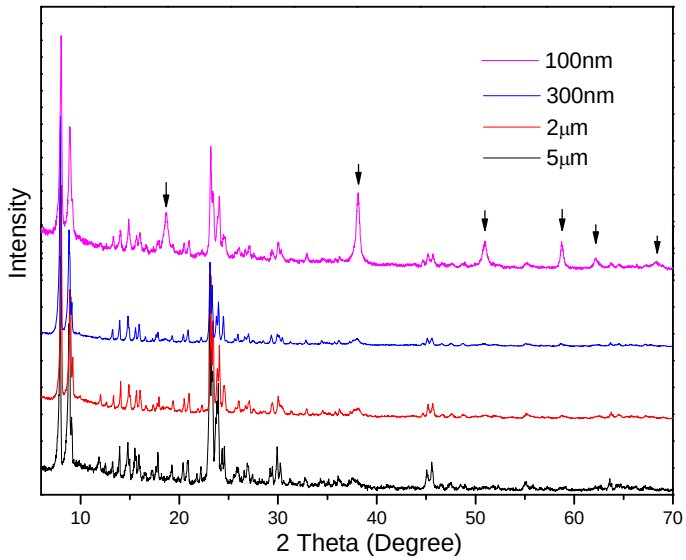

Fig. S4. XRD patterns of MFI particles treated with Grignard reagent; peaks with arrows are from $Mg(OH)_2$. All particles maintained MFI structures after the treatment. In the case of large crystals such as 5 and 2 μm particles, only peaks from MFI were observed due to the high crystallinity of the zeolite. However, as the particle size decreased to 100nm, the peaks from nanocrystals created by the treatment became distinguishable and the positions of the new peaks were well matched with tabulated $Mg(OH)_2$ peaks.

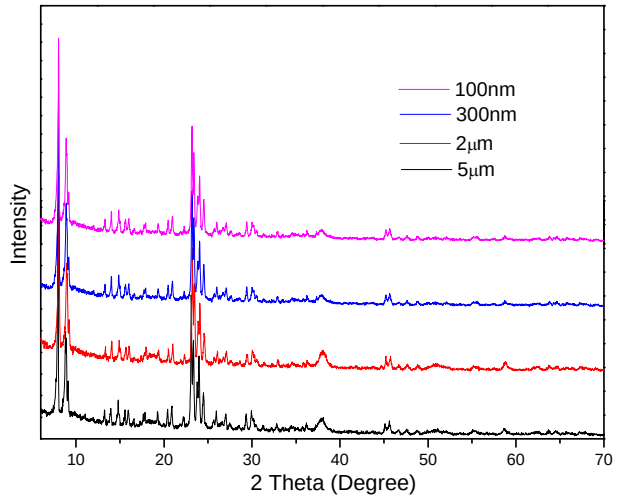

(a)

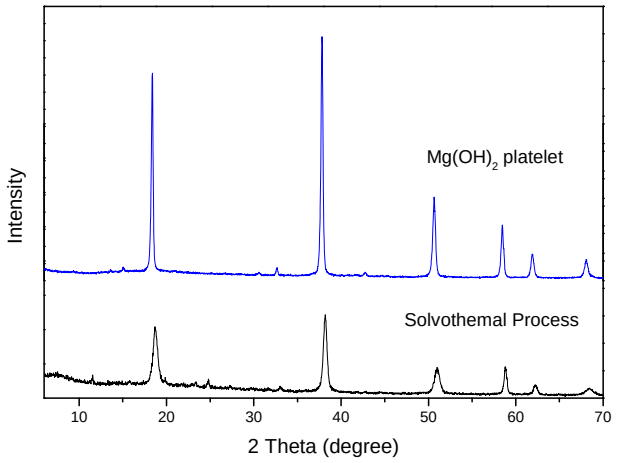

(b)

Fig. S5. XRD patterns of (a) MFI particles solvothermally treated and (b) crystals solvothermally synthesized without zeolites. The peaks from crystalline $Mg(OH)_2$ are weak (e.g., a broad peak at 38° 2θ (Fig. S5 (a)). To identify the structure created from the solvothemal treatment, the crystals were synthesized without MFI particles. As shown in Fig. S5 (b), peak positions were well matched with those of $Mg(OH)_2$. In addition, peak broadening was observed due to the small size of the $Mg(OH)_2$ domains.

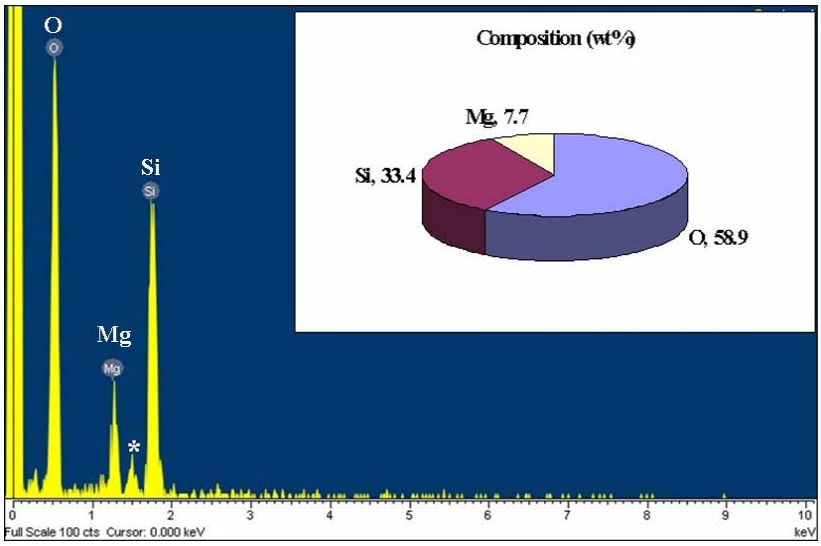

* Aluminum peak from sample mount

Fig. S6. EDS spectrum and elemental composition of solvothermally treated 5 μm MFI. Si, O and Mg are the main elemental components of the sample.

Table S1. Bulk compositions of solvothermally treated MFI measured by ICP-AES. $Mg(OH)_2$ yields were very high (96% or more) so that 8.3- 9.6 wt % of Mg was detected in all cases.

	Mg	Si
100nm	8.3	33.2
300nm	9.6	33.7
2μm	9.2	32.3

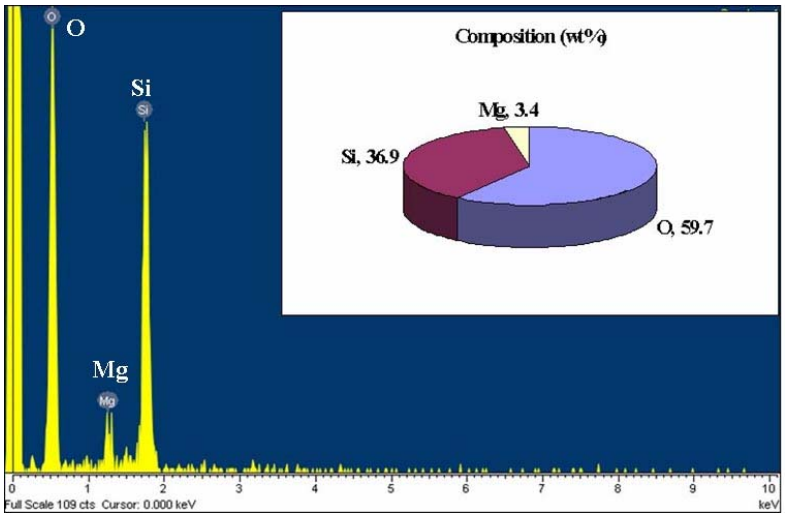

Fig. S7. EDS spectrum and elemental composition of Grignard treated 5 μm MFI. Si, O and Mg are main components of the sample.

Table S2. Bulk compositions of Grignard treated MFI measured by ICP-AES. Mg to Si ratio increased as the particle size decreased. Since 100nm MFI provided the largest surface area, the maximum amount of $Mg(OH)_2$ was formed on the surface. Due to this high $Mg(OH)_2/SiO_2$ ratio, the peaks from $Mg(OH)_2$ were shown in XRD pattern of 100nm MFI.

	Mg	Si	Na
100 nm	15.7	26.1	0.5
300 nm	7.5	36.0	0.2
2 μm	3.5	39.8	0.3

Table S3. External surface area (BET) of untreated and surface-treated MFI crystal. Since there is a strong relationship between the surface roughness and the surface area of a nanostructure, we quantified the roughness effects by measuring the BET external surface area. The MFI crystals used for these measurements were uncalcined (i.e., the organic structure-directing agent remains in the pores), and therefore the zeolite pores make essentially no contribution to the measured surface area.

	300 nm MFI (m^2/g zeolite)	2 μm MFI (m^2/g zeolite)
Untreated	7.5	3.7
Grignard treated	39.8	11.0
Solvothermally treated	74.5	35.1

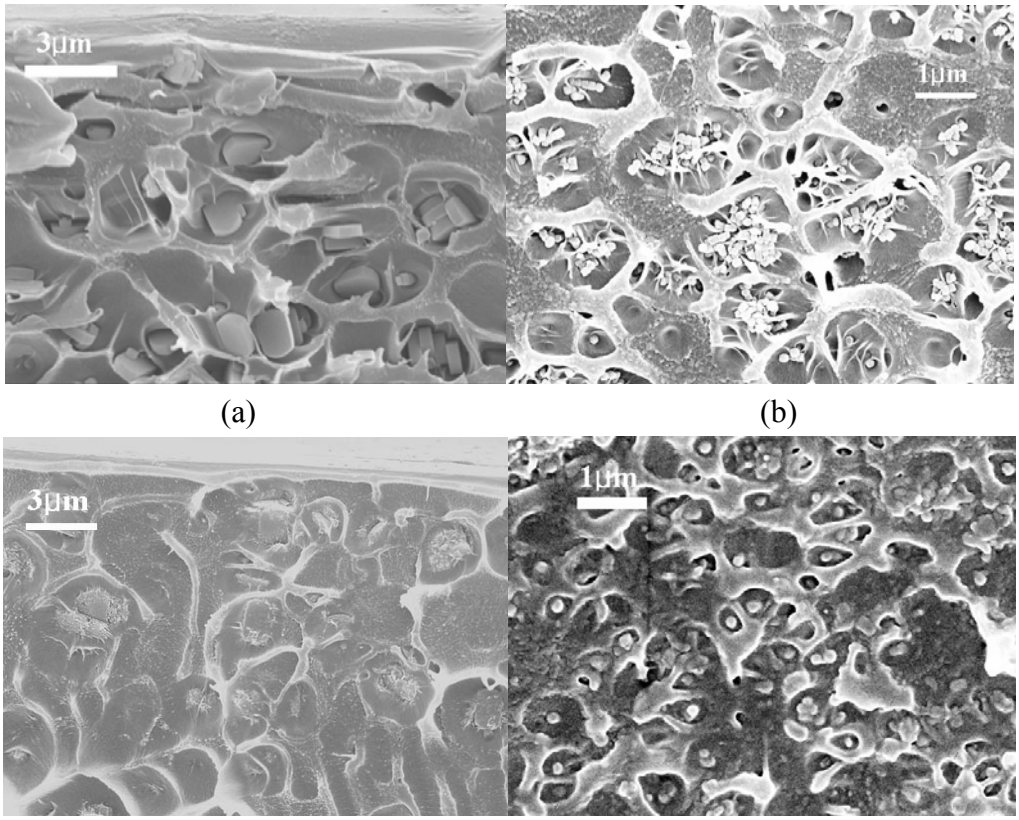

Fig. S8. SEM images of cross-section of mixed matrix dense films made with MFI and Ultem®. (a) 2 μm bare MFI in Ultem®, (b) 100nm bare MFI in Ultem® (c) 2 μm solvothermal treated MFI in Ultem® and (d) 100 nm solvothermal treated MFI. Not only was adhesion between MFI and Ultem® improved, but also the particles were uniformly distributed in the polymer matrix after the solvothermal treatment.

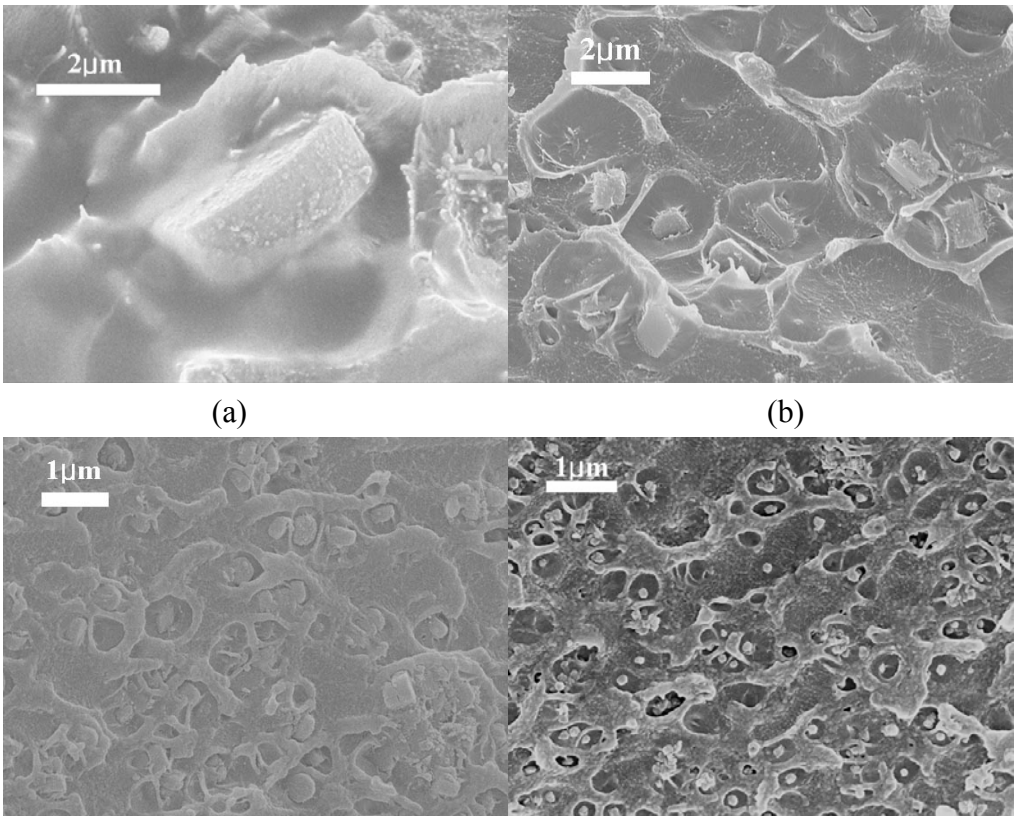

Fig. S9. SEM images of cross section of mixed matrix dense films made with Grignard treated MFI and Ultem®. (a) 5 µm, (b) 2 µm, (c) 300 nm and (d) 100 nm crystals. All membranes also showed good morphology; good zeolite/polymer contact and uniform distribution of particles.

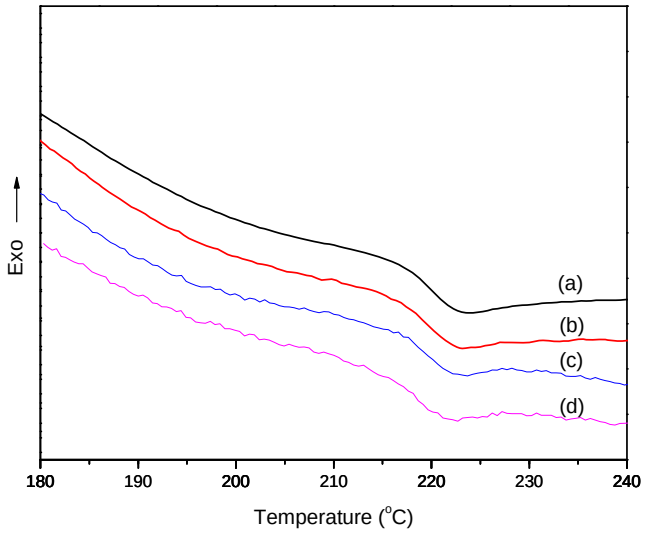

Fig. S10. DSC curves of pure and composite films; 50 wt % of 300 nm MFI loading; (a) pure Ultem®; (b) Bare MFI loading; (c) Grignard treated MFI loading; (d) Solvothermally treated MFI loading. The rigidification of polymer chains at interface region is an important issue, resulting in lower gas permeability than the theoretical estimate. However, in this study, there were no observable changes in the glass transition temperature of poly(etherimide) in the mixed matrix dense films.

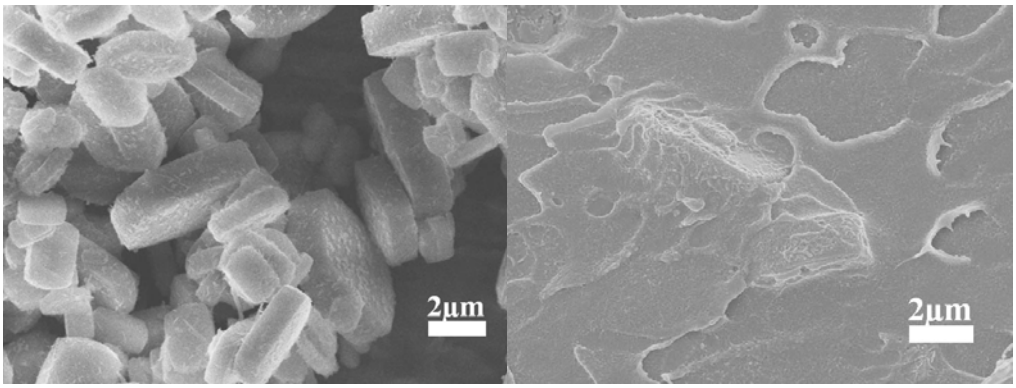

(a) (b)

Fig. S11. Solvothermal-based $Ca(OH)_2$ nanostructure fabrication on the surfaces of pure-silica MFI. (a) surface-treated pure-silica-MFI and (b) cross section of mixed matrix dense film made with surface treated MFI and Ultem®. Roughened surfaces were made by the creation of $Ca(OH)_2$ nanostructure and resultant particles showed improved adhesion with Ultem®.

Table S4. Further Details of Pure-Component Gas Permeation Properties of Matrimid Membranes Containing 300 nm Solvothermally Treated MFI Crystals at 35°C and 2 atm Upstream Pressure. Rows #1 and #3 in the Table (Pure Matrimid and 35 wt% MFI in Matrimid) are reported in Table 1 of the main Communication as examples. Additional results from 20 wt% MFI/Matrimid membranes and control experiments with untreated MFI/Matrmid membranes are also included in the Table below (Rows #2 and #4).

Membrane	*CO_2 permeability (Barrer)*	*CH_4 permeability (Barrer)*	*CO_2/CH_4 selectivity*
Pure Matrimid	7.6±2.3	0.21±0.07	35±1
20 wt% solvo-treated-MFI in Matrimid	23±1	0.59±0.02	39±3
35 wt% solvo-treated-MFI in Matrimid	31±2	0.78±0.04	39±4
20 wt% untreated MFI in Matrimid	42±1	1.5±0.1	28±2

Membranes prepared with solvothermally treated MFI show substantially enhanced performance over pure Matrimid in terms of a very high permeability *and* maintenance of high selectivity. In contrast, membranes prepared with untreated MFI show a much lower selectivity and a very large permeability characteristic of the defective "sieve-in-a-cage" morphology. Further characterization of the solvothernally treated MFI/Matrimid interfaces, as well as further improvements in the membrane selectivity and interface morphologies, are possible and ongoing.

References

(1) Cheng, C. H.; Bae, T. H.; McCool, B. A.; Chance, R. R.; Nair, S.; Jones, C. W. *J. Phys. Chem. C* **2008**, *112*, 3543.

(2) Agger, J. R.; Hanif, N.; Cundy, C. S.; Wade, A. P.; Dennison, S.; Rawlinson, P. A.; Anderson, M. W. *J. Am. Chem. Soc.* **2003**, *125*, 830.

(3) (a) Moore, T. T.; Koros, W. J. *J. Mol. Struct.* **2005**, *739*, 87. (b) Moore, T. T.; Damle, S.; Williams, P. J.; Koros, W. J.; *J. Membr. Sci.* **2004**, *245*, 227.

(4) Chung, T.-S.; Jiang, L. Y.; Li, Y.; Kulprathipanja, S. *Prog. Polym. Sci.* **2007**, *32*, 483.

(5) Mahajan, R.; Koros, W. J. *Polym. Eng. Sci.* **2002**, *42*, 1420.